Soft Matter

Accepted Manuscript

ROYAL SOCIETY OF CHEMISTRY

www.rsc.org/softmatter

Disintegration of protein microbubbles in presence of acid and surfactants: a multi-step process

Tijs A.M. Rovers[a,b], Guido Sala[a,b,c], Erik van der Linden[a,b] and Marcel B.J. Meinders[a,c,*]

[a] Top Institute Food and Nutrition, P.O. Box 557, 6700AN, Wageningen, the Netherlands

[b] Laboratory of Physics and Physical Chemistry of Foods, Wageningen University and Research Centre, P.O. Box 17, 6700 AA, Wageningen, the Netherlands

[c] Food and Biobased Research, Wageningen University and Research Centre, Wageningen, P.O. Box 17, 6700 AA, Wageningen, the Netherlands

[*] Corresponding author, tel: +31 317 480165, e-mail: marcel.meinders@wur.nl

Abstract

The stability of protein microbubbles against addition of acid or surfactants was investigated. When these compounds were added, the microbubbles first released the encapsulated air. Subsequently, the protein shell completely disintegrated into nanometer-sized particles. The decrease in the number of intact microbubbles could be well described with the Weibull distribution. This distribution is based on two parameters, which suggests that two phenomena are responsible for the fracture of the microbubble shell. The microbubble shell is first weakened. Subsequently, the weakened protein shell fractures randomly. The probability of fracture turned out to be exponentially proportional to the concentration of acid and surfactant. A higher decay rate and a lower average breaking time were observed at higher acid or surfactant concentrations. For different surfactants, different decay rates were observed. The fact that the microbubble shell was ultimately disintegrated into nanometer-sized particles upon addition of acid or surfactants indicates that the interactions in the shell are non-covalent and most probably hydrophobic. After acid addition the time at which the complete disintegration of the shell was observed coincided with the time of complete microbubble decay (release of air), while in the case of surfactant addition, there was a significant time gap between complete microbubble decay and complete shell disintegration.

1. Introduction

Protein stabilized microbubbles are micron-sized air bubbles with a relatively thick interfacial layer that makes them stable with respect to disproportionation [1-4]. Conventional ways of making microbubbles include sonication, high shear mixing, template–layer-by-layer deposition and membrane emulsification. Recently, new technologies to produce microbubbles, like microfluidic devices, electrohydrodynamic atomization and pressurized gyration, have been developed [3, 5-10]. Microbubbles are considered as a food ingredient with high potential as fat replacer or for the creation of new textures in foods [11, 12]. Rovers et al. [2] showed that preparation conditions determined yield, size and stability of Bovine Serum Albumin (BSA) microbubbles made by sonication. The stability of microbubbles was related to the interactions that are formed between BSA molecules at the microbubble surface during sonication [1]. The interactions in the microbubble shell and their role for the stability of the microbubbles are subject of debate in literature. Suslick et al. [4] claimed that covalent disulfide bonds between the cysteine residues of BSA molecules are the main interactions in the shell of microbubbles prepared with this protein. Protein microbubbles are mostly made using cysteine-rich proteins, which seems to support this claim. However, it was observed that microbubbles can also be obtained with proteins that have no cysteine residues, implying that other interactions are responsible for the formation and stability of protein microbubbles made by sonication [13]. For polyglutamate microspheres, it was shown that interactions in the shell are non-covalent [14] and according to Cavalieri et al. [1] the interactions in a protein microbubble shell are a combination of covalent bonds and hydrophobic interactions. With this study we aim to get more insight on the nature of the interactions responsible for formation and stability of protein microbubbles. Furthermore, for practical applications, it is very important to get insights on the behaviour of microbubbles in different environments. Some studies on the stability of protein microbubbles under changing environment have already been reported. When subjected to a temperature of 121°C for 15 minutes, BSA microbubbles stayed intact and formed a gel of microbubbles [15]. Microbubbles prepared with BSA and dextrose were stable against ultrasound of 1 MHz and 3 MHz when their size was 1 µm or smaller, while bigger microbubbles were destructed at this high frequency ultrasound [16]. For food applications, insights on the stability of microbubbles in presence of food components are needed. It is has been described that microbubbles were stable for 2 months in the presence of oil droplets [12]. In the current study we investigated the stability of microbubbles made by sonication upon addition of surfactants, more specifically Sodium dodecyl sulphate (SDS), or acid. We aim to relate the stability of the microbubbles to physical phenomena.

2. Materials and methods

2.1 Materials

Bovine serum albumin (BSA, fraction V, lot nrs: 100m1900V, SLBF0550V and SLBC8307V), sodium dodecyl sulphate (SDS) polysorbate 20 (Tween 20), sucrose monolaurate and hydrochloric acid (HCl) were purchased form Sigma-Aldrich (St. Louis, MO, USA). For all experiments demineralized water was used.

2.2 Preparation and washing of microbubble dispersions

Microbubbles were prepared as previously described [2]. In short, 5% (w/w) BSA was dissolved in demineralized water, and the BSA solution was stirred for at least 2 hours. The pH of the solution was adjusted to 6.0 by addition of 2.0 M HCl and 0.2 M HCl. The solution was subdivided in portions of 25 ml, which were transferred to 50 ml beakers. The samples were heated for 10 minutes in a 55°C water bath and subsequently sonicated for 3 minutes at power level 8 and duty 30% cycle (when protein lot nr 100M1900V was used) or 90% duty cycle (when protein lot nr SLBF0550V or SLBC8307V were used), using a Branson 450 sonicator (Branson Ultrasonics Corporation, Danbury, CT) with a 20kHz, 12.7 mm probe. The probe was placed at the air-water interface of the solution.

The microbubble dispersions made with the protein from lot nr SLBF0550V or SLBC8307V contained, besides microbubbles, also protein aggregates. For further experiments, the microbubble dispersions were washed. They were centrifuged for 45 minutes at 400 g. The top layer, mainly consisting of microbubbles, was collected. The remaining dispersion was centrifuged for 45 minutes at 800 g. Also from this dispersion the top layer was collected. The collected top layers were diluted with demineralized water in order to obtain a concentration of microbubbles (number per volume) that was comparable to that of the microbubble dispersion before washing.

2.3 Visualization of microbubble disappearance

The effect of the studied parameters on microbubbles was visualized by taking pictures of microbubble dispersions to which HCl or a solution of SDS was added. One drop of microbubble dispersion was placed on an object glass, which was covered with a cover glass. Subsequently, one drop of 1 M HCl or one drop of a 1% SDS solution was placed just next to the cover glass, allowing the HCl or SDS to diffuse into the microbubble dispersion. The object glass was placed under a phase contrast microscope (Leica Reichert Polyvar, Leica Microsystems, Wetzlar, Germany) or a light microscope (Axioskop, Carl Zeiss AG, Oberkochen, Germany) at a 40x magnification. A camera (MC120 HD, Leica Microsystems,

Wetzlar, Germany or Axiocam HRc, Carl Zeiss AG, Oberkochen, Germany) connected to the microscope took pictures with a time interval of 1 second.

2.4 Determination of microbubbles number and size after acid or surfactant addition

2.4.1 Preparation of the samples

Predetermined volumes of 2 M HCl were added under continuous stirring to the microbubbles dispersions. The exact pH values reached as a result of these additions were noted after the determination of the number or size of the microbubbles.

A stock solution of 2% (w/v) SDS was made and stirred for more than 2 hours. From this stock solution dilutions were made to concentrations that were twice the concentration desired in the final solution. These SDS solutions were mixed 1:1 with the microbubble dispersions and subsequently vortexed for 15 seconds. The final BSA concentration in these microbubble-SDS mixtures was 2.5% (0.376 mM). The final SDS concentrations in the different samples were 0.011% (0.376 mM), 0.044% (1.50 mM), 0.075% (2.60 mM), 0.10% (3.47 mM) and 0.125% (4.33 mM). Therefore, the [SDS]:[BSA] ratios were 1.0, 4.0, 6.9, 9.2 and 11.5. SDS was added to the washed microbubble dispersions, containing 0.89% BSA (0.134 mM) to obtain final concentrations of 0.011% (0.376 mM), 0.022% (0.75 mM), 0.044% (1.50 mM), giving [SDS]:[BSA] ratios of 2.8, 5.6, and 11.2. To compare the effect of SDS to that of other surfactants, also Tween 20 and sucrose laurate were added to unwashed microbubble dispersions at a [surfactant]:[BSA] ratio of 6.9.

2.4.2 Determination of the number of microbubbles

Immediately after stirring or vortexing, one drop (20 µl) of acidified microbubble dispersion or one drop of the microbubble-surfactant mixture was put on the object glass. This was covered by a cover glass. To prevent evaporation, all sides of the cover glass were sealed with Sellotape. Microscope (Axioskop, Carl Zeiss AG, Oberkochen, Germany) images (40x magnification) of one specific spot of the acidified microbubble dispersion or the microbubble-surfactant mixture were taken at standard time intervals with a camera (Axiocam HRc, Carl Zeiss AG, Oberkochen, Germany). From the microscope pictures, the number of microbubbles was estimated by image analysis using ImageJ (1.44n, National Institutes of Health, Bethesda, MD). All experiments were done at least in duplicate.

2.4.3 Determination of the size of microbubbles

The size of microbubbles and microbubbles shell remainders after SDS or HCl addition was measured with dynamic light scattering, using a Zetasizer Nano ZS (Malvern Instruments Ltd, Malvern, United Kingdom).

2.5 Data processing

Data were analysed using Matlab (R2013a, Mathworks Natick, MA, United States) and built-in functions for non-linear fitting. Average breaking times, t_b, were calculated with $t_b = \frac{\sum_1^n(\Delta N_n \cdot t_n)}{\sum_1^n \Delta N_n}$, in which $\Delta N_n = N_n - N_{n-1}$, with N_n and N_{n-1} the number microbubbles on time t_n and t_{n-1}, respectively.

3. Results and discussion

3.1 Stability against acid

3.1.1 Visualization of microbubble disintegration after acid addition

The addition of a drop of 1 M HCl to a microbubble dispersion induced the disappearance of the microbubbles, as can be seen in Fig. 1. The drop of HCl was placed at the left side of the sample. HCl diffused into the dispersion from the left to the right side. The microbubbles disappeared within seconds. The micrographs on the top left, top right, and bottom left of Fig. 1 show pictures made with a normal light microscope at 0, 5, and 10 seconds after addition of the acid. The micrograph at the bottom right of Fig. 1 shows a picture made with a phase contrast microscope. It seems that at the moment the microbubbles came in contact with the concentrated acid solution they disappeared almost immediately. Also, in the micrographs taken with a phase contrast microscope, a front of disappearing white spots was visible that moved from left to right. These white spots corresponded to the air in the intact microbubbles. This means that the microbubbles released their air quickly after the acid reached them. After the release of air, some remainders of the microbubbles were visible (Fig. 1, bottom right). These corresponded to the shells or parts of the shells, which remained after the microbubbles lost their enclosed air. After some time, also the grey spots disappeared (not shown), indicating a complete breakdown of the microbubble shell. The two stages of microbubble disappearance, the release of air and the complete disintegration of the microbubble shell, are described in more detail in the two following paragraphs.

3.1.2 Escape of air from microbubble after acid addition

In this section we will focus on the first part of the microbubble disintegration, i.e. the release of air form the microbubbles. Using a normal bright field microscope the air-filled microbubbles are visible, while water filled microbubbles are not. This allows the determination of the number of microbubbles after addition of acid or surfactant. Fig. 2 shows the relative number of microbubbles measured as a function of time for different changes in pH value, $\Delta pH = pH_{add} - pH_0$, in which pH_{add} is the pH after acid addition and pH_0 is the pH before acid addition, i.e. pH 6.

The time until the number of microbubbles decreased by 50% of the original number ($t_{1/2}$) was above 150 minutes at ΔpH around 2 .0. For ΔpH around 2.7, $t_{1/2}$ turned out to be almost zero. In samples with a lower ΔpH there was a lag time before the microbubbles released the air. This behaviour might be due to the superposition of two phenomena, each with a characteristic time, the first corresponding to a weakening of the protein shell caused by a change in pH, and the second corresponding to the fracture of the weakened shell that could not withstand the Laplace pressure anymore. Therefore, we fitted our data to the univariate Weibull distribution, $e^{-(\alpha t)^{\beta}}$ [17]. The fitted Weibull functions are depicted by the dotted lines in Fig. 2. The parameter β is often called the shape factor and describes the wearing rate of a process. The parameter α represents the Poisson killing rate, the decay rate of the distribution, and corresponds to the average failure time of a stochastic failure process [17-19]. In our case the aforementioned weakening of the shell is described by the wearing rate β. When the shape parameter β is larger than one, a certain lag in the fracture process is observed. In our study the parameter α corresponds to the decay rate of the microbubbles, which describes how fast the shell ruptured upon release of air. The parameters α (on a log-linear scale) and β (on a linear-linear scale) are plotted as function of ΔpH (top graphs of Fig. 3).

For samples with a ΔpH smaller than 2.4, β was slightly larger than 1. This means that at low acid concentrations there is a time lag in the release of air from the microbubble. We hypothesize that the parameter β can be defined by the result of several phenomena that weaken the microbubble shell. One phenomenon that controlled the weakening rate of the shell was the diffusion of acid to and through the microbubble shell, which at lower acid concentration was lower than at high acid concentrations. Subsequently, the addition of acid protonated the BSA molecules in the microbubble shell, making them more positively charged. Higher concentrations of acid resulted in a higher degree of protonation and BSA molecules that were more positively charged, resulting in a larger inter- and intra-molecular repulsion. Furthermore, at pH further away from the isoelectric point (4.7) BSA molecules are

in a more stretched conformation, resulting in a higher excluded volume for every BSA molecule [20]. All these phenomena (diffusion, protonation and resulting repulsion and BSA conformation change) resulted in a weaker shell at higher acid concentrations.

The decay rate α increased exponentially with ΔpH. The decay of the microbubble might be described as a random fracture phenomenon of a hollow sphere with a thin protein shell under constant (Laplace) pressure. In literature random fracture has been described for gels [21]. According to Bonn et al. [21] the random fracture model is only applicable when the fracture has a random nature, which means that the decay can be described as a univariate distribution. Since the parameter α describes an exponential, univariate distribution, the decay of the microbubble shells is assumed to fulfil those criteria. The shell fractured randomly with a higher probability of breaking and a lower average breaking time, t_b, at higher ΔpH (Fig. 3, bottom left). The probability of breaking, and consequently the average breaking time, could be well described by the decay rate α, as shown on the bottom right graph of Fig. 3.

3.1.3 Disintegration of microbubble shell after acid addition

After air release, the remaining shell of the microbubbles (shown in right bottom micrograph of Fig. 1) disappeared, as well. In order to further investigate this, we added acid to the microbubble dispersion and measured the size of microbubbles and remainders in time. In Fig. 4 an example of the measured size distributions is given for an acidified microbubble dispersion at ΔpH 2.19 at different times after acid addition.

The volume-based mean radius of the microbubbles decreased in time to a size of several nanometers. The size of the final particles coincide with that of BSA monomers or dimers. This means that weak acid concentrations can break the intermolecular bonds in the microbubble shell, indicating that the interactions in the microbubble shell are non-covalent. In Fig. 4 a gradual decrease in size of microbubble and microbubble remainders is observed for dispersions with ΔpH 2.19. The time span in which the microbubbles were broken down to nanometers particles was of the same order of magnitude as the time required to break the microbubble shell and release the air in dispersions with ΔpH around 2.3. This can be seen in the bottom left graph of Fig. 2. It suggests that the time between first fracture (leading to the release of air) and subsequent disintegration, leading to breakdown to nanometer particles, was very short. This was also observed at higher values of ΔpH, where the decrease in size was not gradual. In those dispersion the size directly dropped from sizes typical of microbubble to nanometers, suggesting a very short time between first fracture and subsequent disintegration. The parameter β for the decay of the microbubbles upon acid

addition was low. This means that the shell weakened relatively quickly, resulting in a short lag phase and in a shell that quickly disintegrated.

3.2 Stability against surfactants

3.2.1 Visualization of microbubble disintegration after SDS addition

Similar as observed for the experiments with acid, addition of a drop of 1% SDS solution resulted in the disappearance of microbubbles, as can be seen in Fig. 5. The drop of SDS solution was placed at the right side of the sample and SDS was allowed to diffuse from the right to the left side. The micrographs shown in Fig. 5 were made with a phase contrast microscope at three different times after the addition of the SDS solution.

The disintegration of microbubbles by SDS was similar to that observed after acid addition. First the white spots disappeared from the micrographs, which means that the air escaped from the microbubble. Dark spots remained visible, as can be seen in the second micrograph. These dark sports corresponded to the protein shell and/or parts of the shell. After some time the darker spots also disappeared, as can be seen in the third micrograph. This implies a complete disintegration of the microbubble shell.

3.2.2 Escape of air from microbubble after SDS addition

As described for the experiments with acid, we followed the number of microbubbles in time, also after SDS addition. At higher SDS concentrations the number of microbubbles decreased more quickly and it took less time before all microbubbles had disappeared. The decrease in the number of microbubbles due to SDS addition was fitted with a Weibull distribution as well. For all ratios, except for [SDS]:[BSA]=1.0, it was observed that directly after addition of SDS a large fraction of the microbubbles disappeared. The result is that the microbubble cannot be fitted well with the Weibull function. In dispersions to which acid was added such disappearance of a large fraction of microbubbles directly after acid addition was not observed. A difference in preparation was that the latter samples were washed before the addition of acid. Although the reason for washing was to remove the existing protein aggregates from the dispersion, it is very likely that during the centrifugation also the weakest microbubbles were removed. In order to check if this could be a reason for the disappearance directly after addition, we also washed the microbubble used for experiments with SDS. When SDS was added to these washed microbubble dispersions it was observed

that the decay of the microbubbles followed the Weibull distribution quite well. Therefore, it seems that a fraction of the microbubbles in the unwashed microbubble dispersion had weaker shells that were more vulnerable to SDS and disappeared quickly after addition of this surfactant. This fraction could be removed by centrifugation. In the top graphs of Fig. 6 we plotted the parameter α and β as function of the ratio [SDS]:[BSA].

Higher SDS concentrations resulted in larger decay rates. Furthermore, at all concentrations a lag phase was observed before the microbubbles started to fracture, resulting in values of β larger than 1. We propose to describe the fracture of the microbubbles shell and the subsequent release of air due to SDS addition by the two aforementioned steps. First, SDS weakened the microbubble shell. Phenomena that controlled the weakening of the shell upon SDS addition include diffusion of SDS to and through the microbubble shell and interactions of SDS with the hydrophobic patches of the proteins, thereby weakening the hydrophobic protein-protein interactions in the shell. Secondly, the weakened shell was not able to withstand the Laplace pressure anymore and therefore fractured, a phenomenon that could be described as a random process. Probability of fracture increased with increasing SDS concentrations. With a high probability of fracture, the average breaking time, t_b, is lower and the decay α rate is higher. This can be seen in the bottom graphs of Fig. 6 in which the natural logarithm of t_b is plotted against the ratio [SDS]:[BSA] and against the negative natural logarithm of α.

3.2.3 Comparison between surfactants

We compared the microbubble instability caused by the addition of SDS to the instability caused by other surfactants. The breakdown followed the same pattern; release of air followed by a complete disintegration of the shell (results not shown). For the first phase (release of air) the relative number of microbubbles was plotted as function of time. These microbubbles were not washed. No large decrease in the number of microbubbles was observed directly addition of 2.6 mM surfactant. Also for these samples, the decay pattern could be well described by the Weibull distribution.

We studied microbubble decay by surfactants with the same hydrophobic tail (laurate), but differing in the hydrophilic head group. We assume that the disintegration caused by the other surfactants followed the same pattern as the disintegration caused by SDS: after the surfactants had diffused to and through the shell and adhered to the BSA molecules, the shell was weakened and subsequently fractured randomly. Parameter β was around 1 for all surfactants (results not shown) indicating that at the used concentration the fracture started immediately after the addition of surfactant without any lag phase. The decay rate α was for

sucrose laurate, Tween 20 and SDS, 0.49, 0.10, and 0.029, respectively. No clear relation between surfactant properties, such as critical micelle concentration (CMC), molecular weight (M), hydrophilic-lipophilic balance (HLB), and fracture properties could be identified. The reason for difference in fracture behaviour due to different surfactants should be topic of further research.

3.2.4 Disintegration of microbubble shell after SDS addition

After release of air from the microbubbles (second micrograph of Fig. 5), the remaining shell seemed to disappear as well (third micrograph of Fig. 5). In order to further investigate this, we added SDS to the microbubble dispersion, and measured the size of microbubbles and remainders by dynamic light scattering.

As observed for the disintegration of the microbubble shell by acid, the size of the final particles was comparable to that of BSA monomers or dimers. This means that SDS was able to break down (most of) the bonds in the microbubble shell. This confirms that the interactions in the microbubble shell are non-covalent, since SDS is not able to break covalent bonds. Both ionic as non-ionic surfactants could disintegrate microbubbles. Therefore, the interactions between proteins in the microbubble shell are believed to be of hydrophobic nature. SDS, Tween 20 and sucrose laurate can bind to the hydrophobic patches s of the BSA, with binding energies of around 30 kJ/mol in all cases [22-25].

Fig. 7 shows the average sizes of microbubbles and their remainders function of time after SDS was added for different [SDS]:[BSA] ratios.

At higher surfactant-protein ratios and higher temperature the complete disintegration of the shell occurred faster. After the microbubbles had lost their air, the size of the remainders kept increasing for quite some time, after which the microbubble shells completely disintegrated. This pattern is different from the disintegration of the shells after the addition of acid. In those samples the disintegration of the shell happened shortly after the microbubbles lost their air. The parameter β for the decay of the microbubbles with surfactant was relatively high, implying a relatively slow weakening of the shell and long lag phase. This also resulted in a long time between the first fracture (with subsequent release of air) and the complete shell disintegration. After the microbubble had lost its air, the shell was still present and this water-filled shell appeared to be larger than the air-filled shell, as also can be seen in a microscopy picture of a sample to which SDS was added (Fig. 8).

4. Conclusion

The disintegration pattern of microbubbles upon surfactant or acid addition appears to be similar. Three different steps can be identified. The disintegration of the microbubble, where air dissolves quickly, can be well described with the two-parameter Weibull process. This suggests two processes: 1) a shell-weakening process and 2) a random fracture of the weakened shell. Subsequently, 3) the shell disintegrates completely into monomeric proteins. . For low changes in acid concentrations and all surfactant concentrations, a lag phase is observed in the microbubble decay, indicating that the weakening time is comparable to the breaking time. This is also implied by the Weibull shape factor β being larger than 1. Decay rates (α) increase exponentially and average breaking times (t_b) decrease exponentially with increasing concentrations of acid or surfactant. This means that the probability of a random fracture is larger at a large change in acid or surfactant concentration. During the second step of the microbubble disintegration, the microbubble disintegrates into nanometer-sized protein particles. This means that the bonds between BSA molecules in the microbubble shell can be broken by acid and by ionic as well as non-ionic surfactants. This implies that the interactions in the shell are non-covalent, and most probably hydrophobic. Bonds between the proteins can be broken because surfactants occupy the hydrophobic patches of the BSA molecules in the shell, or because acid changes the conformation and charge of the BSA molecule.

References

1. Cavalieri, F., et al., *Ultrasonic synthesis of stable, functional lysozyme microbubbles.* Langmuir, 2008. **24**(18): p. 10078-10083.
2. Rovers, T.A.M., et al., *Temperature is key to yield and stabilty of BSA stabilized microbubbles*. 2015, accepted in Food Hydrocolloids.
3. Stride, E. and M. Edirisinghe, *Novel microbubble preparation technologies.* Soft Matter, 2008. **4**(12): p. 2350-2359.
4. Suslick, K.S., et al., *Characterization of sonochemically prapared proteinaceous microsperes.* Ultrasonics Sonochemistry, 1994. **1**(1): p. S65-S68.
5. Ekemen, Z., et al., *Fabrication of Biomaterials via Controlled Protein Bubble Generation and Manipulation.* Biomacromolecules, 2011. **12**(12): p. 4291-4300.
6. Elsayed, M., J. Huang, and M. Edirisinghe, *Bioinspired preparation of alginate nanoparticles using microbubble bursting.* Materials Science and Engineering: C, 2015. **46**(0): p. 132-139.
7. Lee, M., et al., *Stabilization and fabrication of microbubbles: applications for medical purposes and functional materials.* Soft matter, 2015. **11**(11): p. 2067-79.
8. Mahalingam, S., M.B.J. Meinders, and M. Edirisinghe, *Formation, Stability, and Mechanical Properties of Bovine Serum Albumin Stabilized Air Bubbles Produced Using Coaxial Electrohydrodynamic Atomization.* Langmuir, 2014. **30**(23): p. 6694-6703.
9. Mahalingam, S., et al., *Formation of Protein and Protein–Gold Nanoparticle Stabilized Microbubbles by Pressurized Gyration.* Langmuir, 2015. **31**(2): p. 659-666.
10. Mohamedi, G., et al., *Effects of Gold Nanoparticles on the Stability of Microbubbles.* Langmuir, 2012. **28**(39): p. 13808-13815.
11. Tchuenbou-Magaia, F.L., et al., *Suspensions of air cells with cysteine-rich protein coats: Air-filled emulsions.* Journal of Cellular Plastics, 2011. **47**(3): p. 217-232.
12. Tchuenbou-Magaia, F.L. and P.W. Cox, *Tribological study of suspensions of cysteine-rich protein stabilized microbubbles and subsequent triphasic A/O/W emulsions.* Journal of Texture Studies, 2011. **42**(3): p. 185-196.
13. Avivi, S. and A. Gedanken, *S-S bonds are not required for the sonochemecial formation proteinaceous microspheres: the case of streptavidin.* Biochemical Journal, 2002. **366**: p. 705-707.
14. Dibbern, E.M., F.J.J. Toublan, and K.S. Suslick, *Formation and characterization of polyglutamate core-shell microspheres.* Journal of the American Chemical Society, 2006. **128**(20): p. 6540-6541.
15. Tchuenbou-Magaia, F.L., I.T. Norton, and P.W. Cox, *Microbubbles with protein coats for healthy food air filled emulsions*. Gums and Stabilisers for the Food Industry 15, ed. P.A. Williams and G.O. Phillips. 2010, Cambridge: Royal Soc Chemistry. 113-125.
16. Borrelli, M.J., et al., *Production of uniformly sized serum albumin and dextrose microbubbles.* Ultrasonics Sonochemistry, 2012. **19**(1): p. 198-208.
17. Weibull, W., *A statistical distribution function of wide applicability.* Journal of Applied Mechanics-Transactions of the Asme, 1951. **18**(3): p. 293-297.
18. Lu, C., R. Danzer, and F.D. Fischer, *Fracture statistics of brittle materials: Weibull or normal distribution.* Physical Review E, 2002. **65**(6): p. 067102.
19. Rinne, H., *The Weibull Distribution: A handbook*. 2008: Chapman and Hall/CRC.
20. Noskov, B.A., et al., *Bovine Serum Albumin Unfolding at the Air/Water Interface as Studied by Dilational Surface Rheology.* Langmuir, 2010. **26**(22): p. 17225-17231.
21. Bonn, D., et al., *Delayed fracture of an inhomogeneous soft solid.* Science, 1998. **280**(5361): p. 265-267.
22. Chakraborty, T., et al., *Physicochemical and Conformational Studies on BSA-Surfactant Interaction in Aqueous Medium.* Langmuir, 2009. **25**(5): p. 3062-3074.
23. Hoffmann, C., et al., *Insights into protein-polysorbate interactions analysed by means of isothermal titration and differential scanning calorimetry.* European Biophysics Journal with Biophysics Letters, 2009. **38**(5): p. 557-568.
24. Makino, S., S. Ogimoto, and S. Koga, *Sucrose monoester of fatty acids - Their properties and interaction with proteins.* Agricultural and Biological Chemistry, 1983. **47**(2): p. 319-326.
25. Nielsen, A.D., K. Borch, and P. Westh, *Thermochemistry of the specific binding of C12 surfactants to bovine serum albumin.* Biochimica Et Biophysica Acta-Protein Structure and Molecular Enzymology, 2000. **1479**(1-2): p. 321-331.

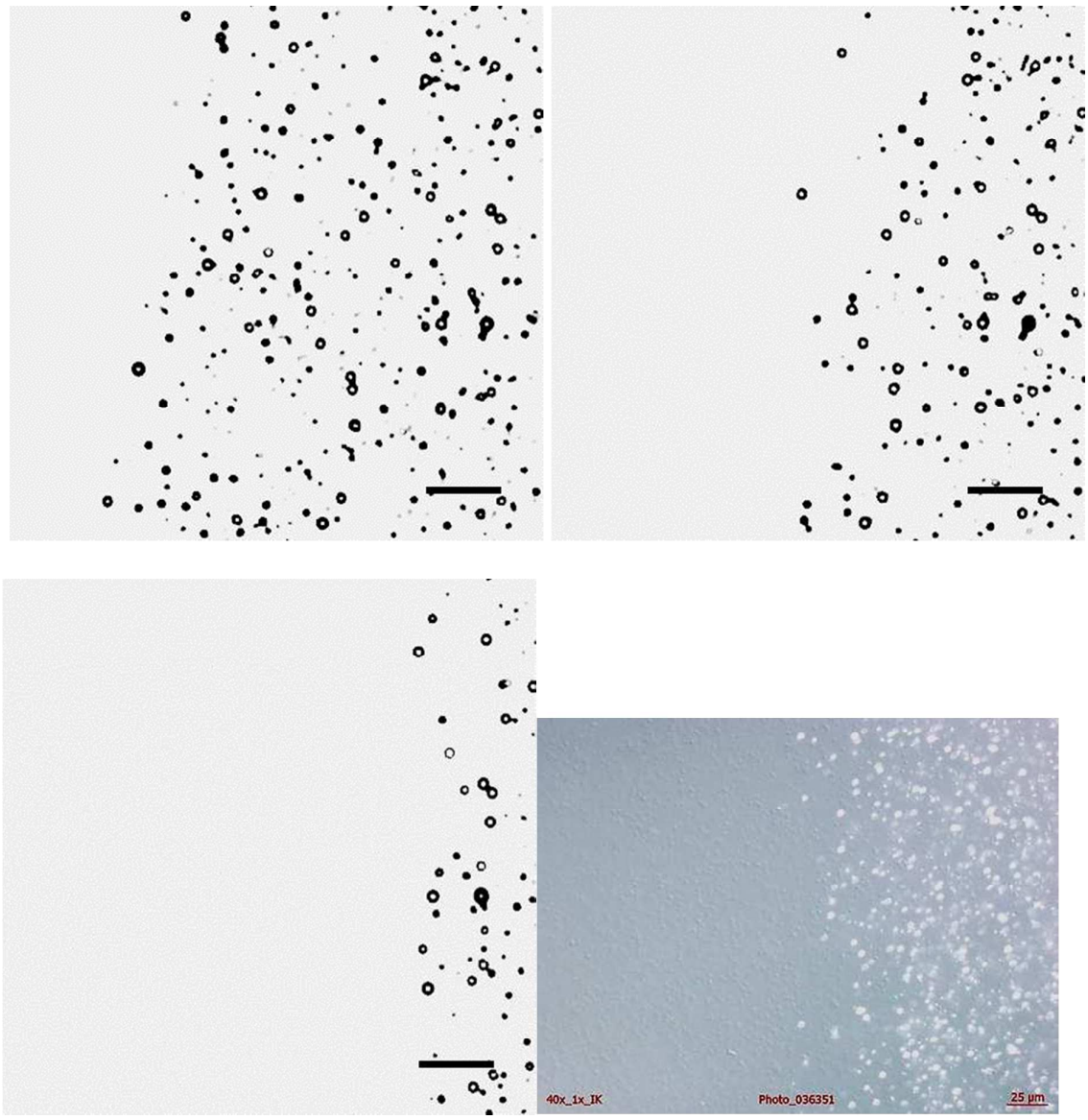

Fig. 1. Micrograph of microbubble dispersion to which at the left side a 1 M HCl solution is added. Micrographs taken with a normal light microscope at different time points: t=0 s (top left), t=5 s (top right), t =10 s (bottom left) with a scale bar of 10 µm. Micrograph taken with a phase contrast microscope, in which the white spots correspond to the intact microbubbles and the grey irregular shaped objects correspond to the remaining broken shell (bottom right) with a scale bar of 25 µm.

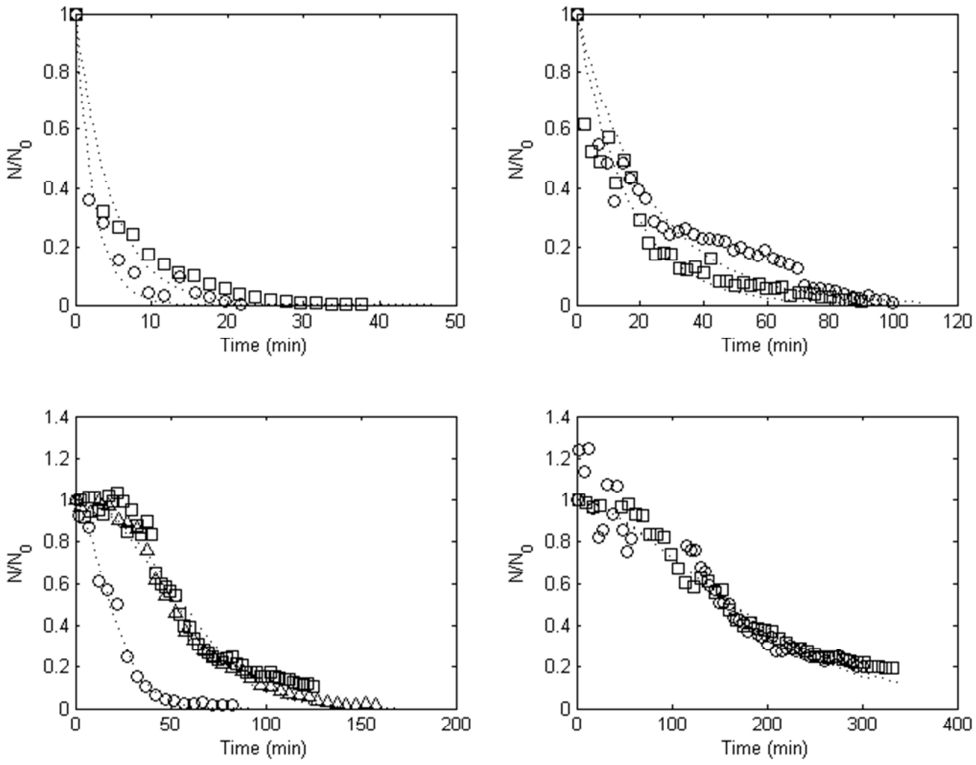

Fig. 2. N/N_0, with N and N_0 being the number of microbubbles at time t and time t=0, as function of the time after addition of HCl for different ΔpH: top left: 2.68 (circles) and 2.66 (squares), top right: 2.46 (circles and squares), bottom left: 2.37 (circles), 2.33 (squares) and 2.29 (triangles),bottom right: 2.05 (circles) and 1.91 (squares). The data are fitted with the Weibull distribution, depicted with the dotted lines.

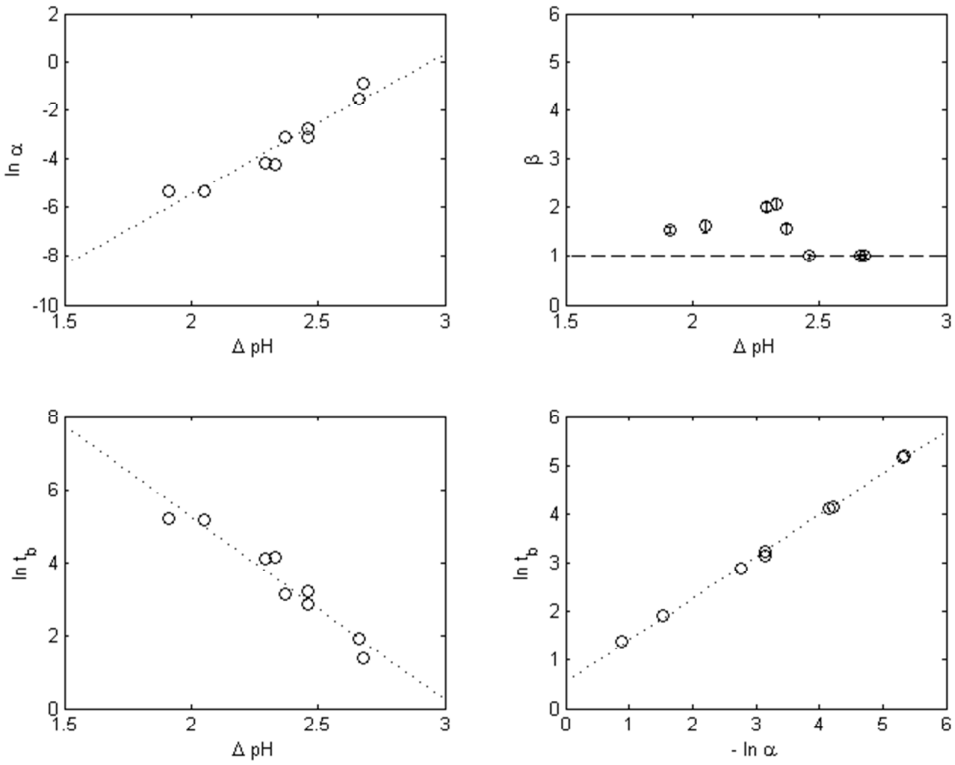

419

420 *Fig. 3. Natural logarithm of parameter α as function of ΔpH (top left), and parameter β as function of the ΔpH (top*
421 *right). Natural logarithm of the average breaking time, t_b, as function of ΔpH (bottom left) and as function of the*
422 *negative natural logarithm of parameter α (bottom right).*

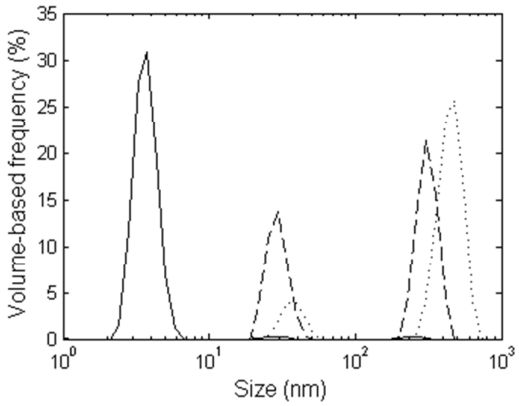

Fig. 4. Volume-based size distribution of an acidified microbubble dispersion with ΔpH 2.19, after 0 minutes (dotted line), 18 minutes (dashed line) and 62 minutes (solid line) on linear-log scale.

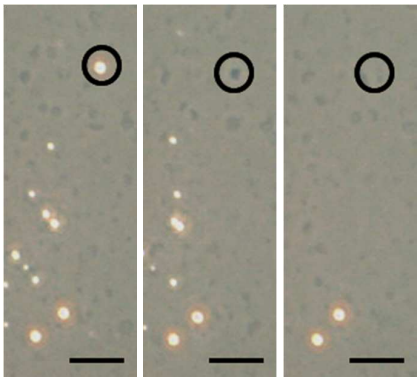

Fig. 5. Micrographs of a microbubble dispersion to which at the right side a 1% SDS solution was added. Micrographs from the phase contrast microscope taken at different time points: t=0 s (left), t=2 s (middle), t =10 s (right). The encircled part shows a typical example of the breakdown process with from left to right: a white spot (corresponding to a microbubble), a dark grey spot (corresponding to the remaining shell) and no spot. Scale bar is 10 µm.

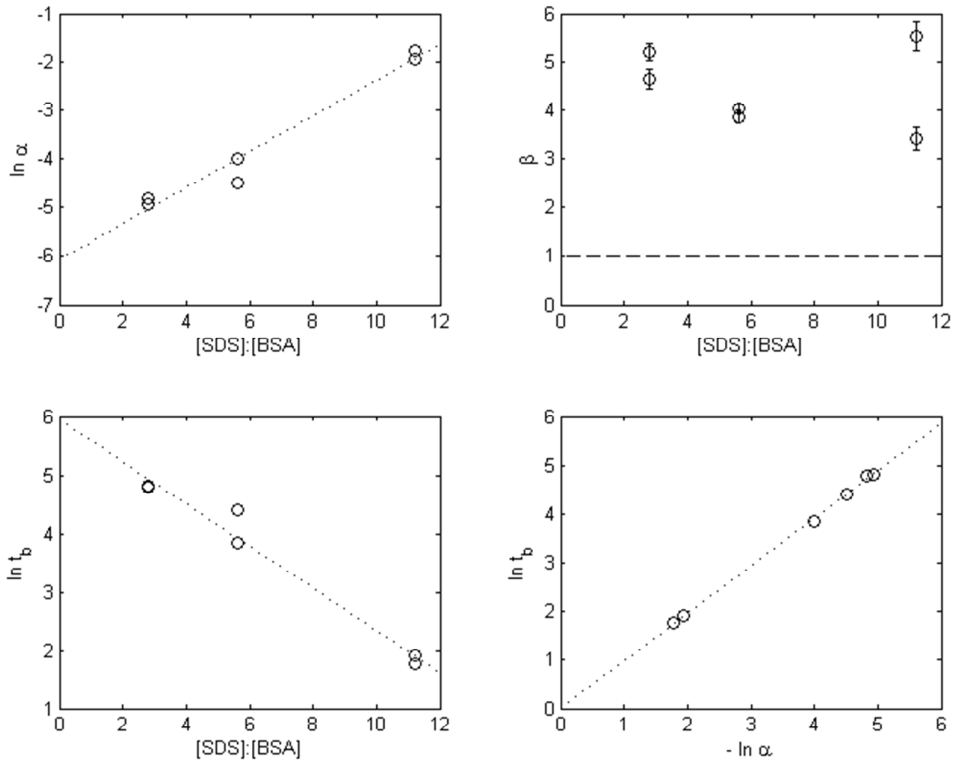

Fig. 6. Natural logarithm of parameter α as function of the ratio [SDS]:[BSA] (top left), and parameter β as function of the ratio [SDS]:[BSA] (top right). Natural logarithm of the average breaking time, t_b, as function of the ratio [SDS]:[BSA] (bottom left) and as function of the negative natural logarithm of α (bottom right).

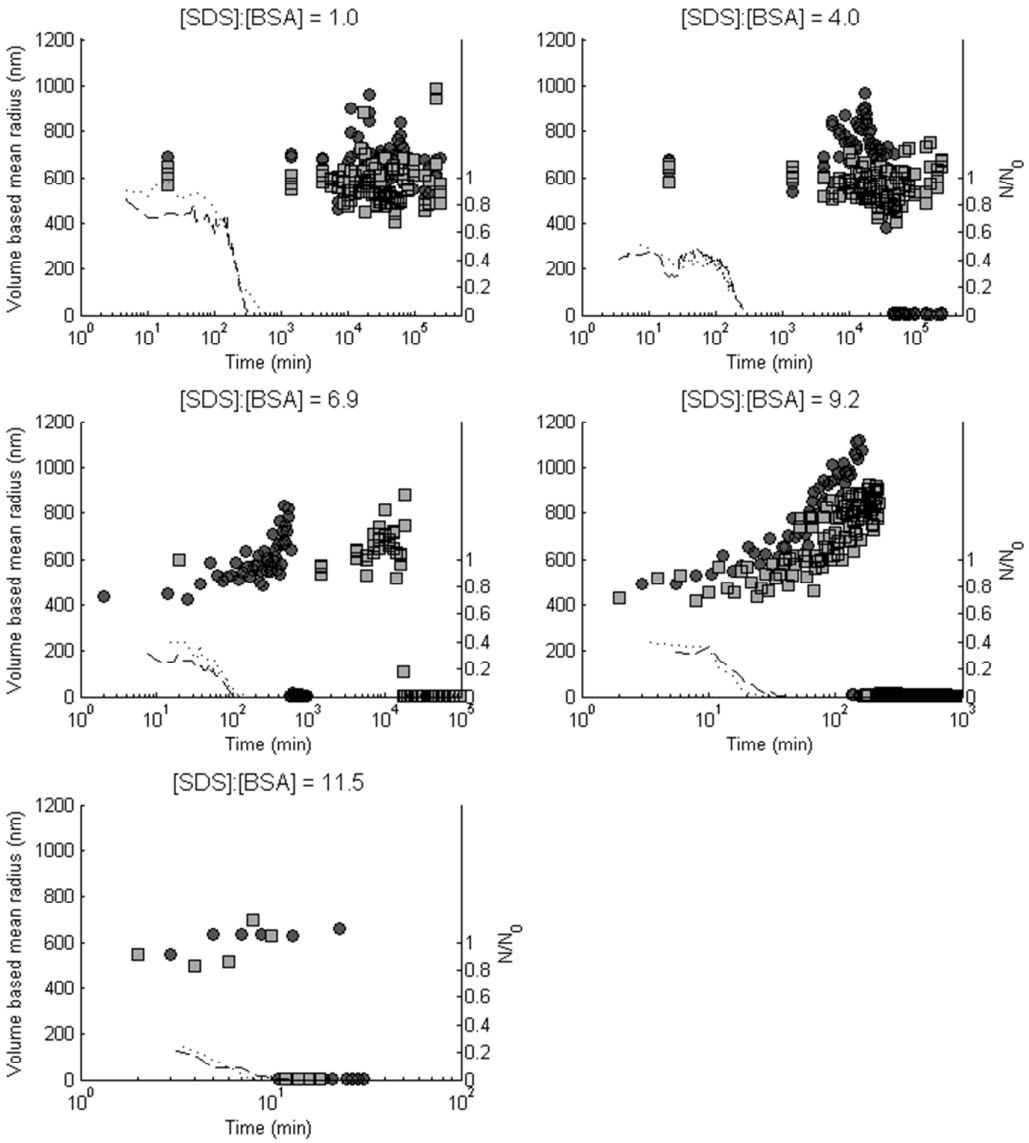

436

437 *Fig. 7. Volume-based mean radius of microbubbles and microbubbles remainders as function of the time after*
438 *addition of SDS for different [SDS]:[BSA] ratios: 1.0 (top left), 4.0 (top right), 6.9 (middle left), 9.2 (middle right)*
439 *and 11.5 (bottom left) on linear-log scale. Sizes are measured for samples at 4°C (squares) and room*
440 *temperature (circles). The dashed and dotted lines represent the decay in the number of microbubbles.*

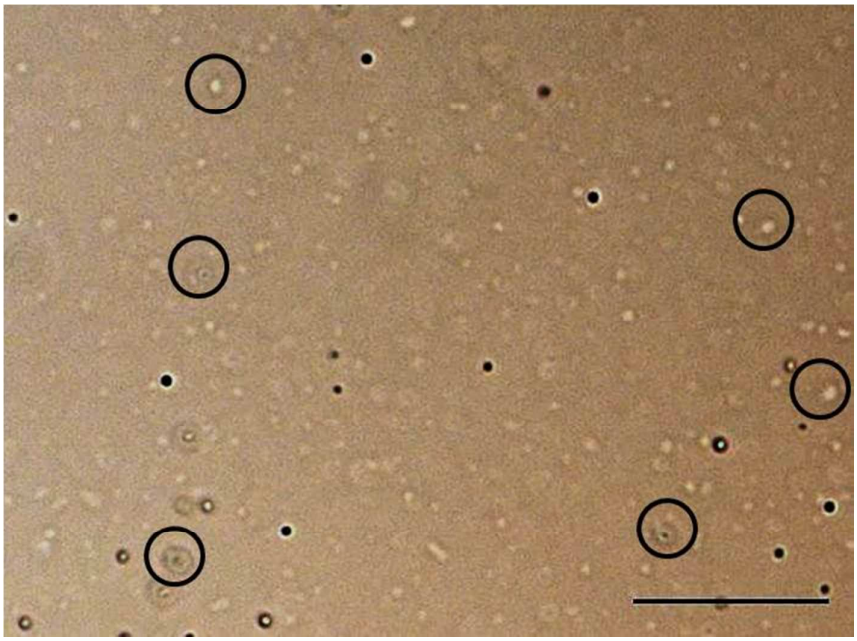

Fig. 8. Micrograph of a microbubbles dispersion to which SDS was added at [SDS]:[BSA] ratio of 9.2 after 38 min (i.e. just before the microbubble size dropped to nanometers). The black dots correspond to the microbubbles. The encircled particles correspond to the remainders of the microbubbles after air release. Scale bar is 25 μm.

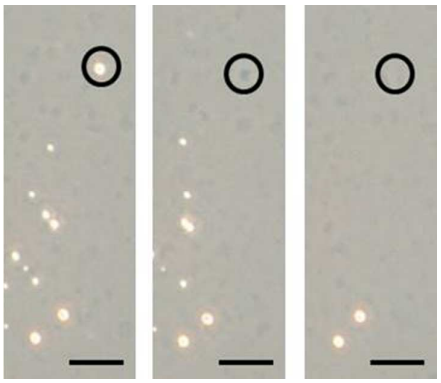

In this manuscript we investigated the stability of microbubbles upon addition of surfactants, (especially SDS) and acid. We related the stability of the microbubbles to physical processes.